

# The impact of mobility model on handover rate in heterogeneous multi-tier wireless networks

Mahmoud Khaki, Abdorasoul Ghasemi\*

*Faculty of Computer Engineering, K. N. Toosi University of Technology, Tehran  
1631714191, Iran*

---

## Abstract

Heterogeneous multi-tier wireless networks deploy many small cells to overcome the scarcity of bandwidth for broadband wireless access. However, increasing the number of cells increases the required handover rate as a mobile user passes through the boundaries of these cells leads to more signaling overhead. We address the impact of mobile users' mobility model in the urban areas on the handover rate. We use two real data sets to model the mobility pattern of pedestrians and drivers, considering their different velocity, move length, and pause time distributions. We use Poisson Point Processes to model the spatial distribution of base stations and assume that the number of handovers is equal to the number of times the users' trajectories cross the cell's boundaries. We derive the distribution function of the handover rate by using the distribution function of the velocity of users. Simulation results are provided to justify the deployed mobility model and the derived analytical results for the handover rate. We find that while the trend of the handover rate against the density of base stations and bias values at different tiers deploying the derived realistic mobility models and simple random waypoint model is the same, the total number of handovers in the network has different behavior. Interestingly, we found that if the number of users increases beyond a threshold, the handover rate decreases, suggesting that the hand over rate is bounded.

---

\*Corresponding author

*Email address:* [arghasemi@kntu.ac.ir](mailto:arghasemi@kntu.ac.ir) (Abdorasoul Ghasemi)

*Keywords:* heterogeneous wireless networks, handover rate, mobility model

---

## 1. Introduction

The ever-increasing of new demands for wireless broadband access could not be met by using traditional methods like increasing the frequency range or the number of base stations [1]. For example, to respond to the forecasted demand  
5 by increasing the frequency spectrum, we need a 1000x spectrum; means using the frequency waves at the limit of visible light [2]. The multi-tier heterogeneous wireless networks (HWNs) emerge as a new solution in which small cells, along with the macrocells, are deployed to provide high access bandwidth for mobile types of equipment. Deploying a large number of smaller cells relief the scarcity  
10 of frequency spectrum; however, the possible movement of users and the passage between these small cells may cause a sharp increase in the total rate of network handover. On the other hand, in HWNs, the commissioning and installation of small base stations (BSs) are done by individuals in private networks in an ad hoc manner that offers services to other users, making the shape of cells  
15 different from the regular ones usually observed in traditional cellular networks. In Fig.1, we show a typical regular network against a two-tier and three-tier HWNs assuming for simplicity that all macro, pico, and femtocells have the same transmission power and bias values.

The irregular cell shapes and the stochastic mobility model of users make  
20 the handover rate estimation an essential and challenging issue in HWNs, which needs need new analytical tools beyond the classical Euclidean geometry like stochastic geometry.

This work addresses the handover rate analysis in multi-tier HWNs. The handover rate plays an essential role in resource management of wireless net-  
25 works and is a determining factor for the signaling overhead. Network operators are interested in decreasing the handover rate by proper mechanisms in the design and operation of networks. Therefore, modeling and estimating the handover rate and its relationship with different parameters like the number of

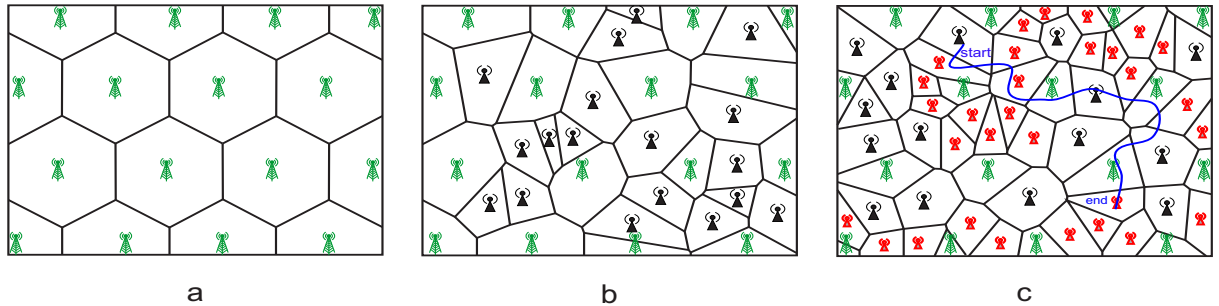


Figure 1: Due to ad hoc small base stations' deployment, the cells' shapes in multi-tier HWN are irregular, causing the handover rate estimation a challenging problem. (a) a typical regular network, (b) a 2-tier network consists of macro and picocells, (c) a 3-tier network consists of macro, pico, and femtocells. The blue line shows a typical user movement trajectory in the network crossing different cells at different tiers.

tiers or the bias values in HWNs is an important research question that needs  
 30 more attention. In multi-tier HWNs, handover management deals with intra-  
 and inter-handovers. The intra- or horizontal handover occurs between two base  
 stations (BSs) at the same tier, and the inter- or vertical handover occurs be-  
 tween two BSs at different tiers [3]. Note that inter-handover management is  
 more challenging and may incur more signaling overhead on the network and  
 35 adverse effects on the user quality of service (QoS) [4]. The network operators  
 are interested in minimizing inter-handovers when a mobile user crosses different  
 cells.

In the following, we summarize some related works on estimating the hand-  
 over rate in HWNs.

40 In [5], the authors deploy the stochastic geometry analysis to analyze the  
 handover rate in a single-tier network. The authors assumed that the BSs are  
 spatially distributed according to the Poisson Point Process (PPP) distribution,  
 and hence the cells' shapes are given by the Poisson Voronoi diagram. The user's  
 mobility model is a modified random waypoint (RWP) model in which each user  
 45 moves at a random speed according to uniformly distributed random variables  
 in a given interval. Next, the handover rate analysis for different path lengths  
 of users and different BSs intensity is performed. The authors show that the

rate of handover in a heterogeneous network is higher than that of a regular hexagonal network.

50 The handover rate analysis for multi-tier networks is discussed in [4] by modeling the spatial distribution of BSs by the PPP and assuming that users move between five random waypoints at a constant speed in the network. The results show that in multi-tier networks, with increasing the number of BSs in a tier, the intra-handover at that tier and the inter-handover with other tiers increases, 55 respectively, almost linearly and logarithmically. In other words, if the network contains  $K$  tiers, increasing the number of BSs of tier- $i$ , the number of handovers between cells in tier- $i$  increases linearly, and the number of handovers between tier- $i$  cells and the cells in other tiers increases logarithmically. Also, the number of handovers in other tiers decreases. To consider the non-uniform 60 spatial distribution of BSs, the authors in [6] suggest the Poisson Cluster Process, which can generate areas in the network with high concentrated BSs. The hand over rate analysis for these networks shows approximately similar results to [4]. In this paper, we show that this result is valid for certain speed limits and the number of users.

65 Assuming homogeneous PPP, the authors in [7] use stochastic geometry tools to evaluate the hand over rate by analyzing a single cell. It is shown that the hand over rate increases logarithmically as the density of BSs or the speed of users increases. The authors did not consider the effect of the number of users and assumed a simple mobility model that does not capture the real scenarios 70 of movements.

The tradeoff between the handover rate and the expected data rate is investigated in [8]. The authors consider a homogeneous single-tier network in a stochastic geometry framework. The mobile user equipment moves according to the RWP model and at a constant speed. The authors find that the expected downlink data rate for the user incurs handovers when crossing the cell's 75 boundary is invariant compared to the mobile user, which does not experience any handover during fixed time periods.

Ref. [9] extends the results of [4] by studying the handover analysis for

networks in a 3-dimensional environment, taking into account the length of  
80 the antennas. The authors considered a heterogeneous network in which the  
base stations are distributed as a Poisson Point Process and assumed that users  
move horizontally at a certain height with the RWP model. Using the stochastic  
geometry framework, the authors estimated the handover rate for Unmanned  
Aerial Vehicles (UAVs).

85 In [10], a new method for estimating the handover rate using the Euclidean  
geometry is proposed. The authors considered a two-tier network consisting  
of macrocells and small cells. The small cells with radius  $r$  and with specified  
intensity are distributed as PPP in the network. The authors estimated the  
inter-handover rate using Euclidean geometry, assuming that the users move  
90 directly in an area with a radius of  $R$ .

In [11], the authors exploited the handover rate in the heterogeneous cellular  
network to estimate UAV's velocity. The results suggest that handover analysis  
has applications in estimating mobile users' velocities without using the global  
positioning system, which decreases the energy consumption of nodes.

95 In this work, we first focus on deriving a more realistic but tractable mo-  
bility model for users due to the strong impact of the user's mobility model on  
handover analysis. We perform data analysis on real traces of pedestrian and  
driver mobility patterns to derive and use a more realistic mobility model in  
our analysis. Interestingly, we found that the handover rate is not an increasing  
100 function of the number of users. This result is reasonable in high-crowded ur-  
ban areas because mobile users' mobilities are restricted as the number of users  
increases. We show that the handover rate does not increase linearly as the  
number of users increases, and there is a non-linear relationship between the  
network handover rate and the number of users. This result has implications  
105 for network operators to manage their resources in dense urban areas.

The rest of the paper is organized as follows. In Section 2, we present  
the system model and problem statement. Section 3 provides data analysis  
on the real mobility traces of pedestrians and drivers in the urban areas to  
derive representative mobility models. Using these modified mobility models,

110 we present the handover rate analysis in Section 4. Simulation results and discussions are provided in Section 5 before concluding the paper in Section 6.

## 2. System Model and Problem Statement

We use the expanded state of the standard Voronoi Poisson diagram, which propose to model a random heterogeneous network in [5]. BSs are distributed  
 115 in  $K$  tiers. In the expanded version, the BSs of tier- $k$  are distributed as an independent homogeneous PPP with parameter  $\lambda_k$ , which is a representative value for the average number of users [12].  $P_k$  denotes the transmission power of the BSs of tier  $k$ ,  $k \in \{1, 2, \dots, K\}$ .

In this model, instead of determining the precise location of BSs, a PPP is  
 120 used in conjunction with specific parameters [13]. The main advantage of this model is that the locations of BSs are independent of each other, and this allows us to analyze network performance with stochastic geometry tools [14, 15, 16]. In PPP spatial distribution, we first generate a random sample of the Poisson distribution with mean  $\lambda_k$ , which determines the number of BSs or users in the  
 125 tier- $k$ . By changing this parameter, we can model dense or sparse networks. Next, the location of each BS is given by randomly and uniformly distributed coordinates in the dimensions of the desired range of the network [4].

We can use a bias coefficient to better manage the intensity of users in each tier or capture various scales of different cell sizes. Typically, users are associated  
 130 with BSs that provides the largest received power; however, by using the bias coefficient, user associates to the BS that provides the largest biased received power [17, 18, 19]. That is, if the user equipment is located at point  $y$ , it selects the  $\mathcal{BS}(y)$ , which provides the maximum biased received power. That is,

$$\mathcal{BS}(y) = \operatorname{argmax}_{x \in \Phi_k, \forall k} \frac{1}{\alpha} B_k P_k |x - y|^{-\gamma}, \quad (1)$$

where  $\Phi_k$  is the corresponding PPP of tier- $k$  BSs, and  $\alpha$  and  $\gamma > 2$  are, respectively, the factor of system losses and the path loss exponent. Note that  
 135  $\frac{1}{\alpha} P_k |x - y|^{-\gamma}$  is the average received power from a BS in tier- $k$  that located in  $x$ ,

and  $B_k$  is the associated bias of tier- $k$ . Biasing facilitates load balancing when we can logically move users from dense tiers to the sparse tiers by increasing the level of bias [2], noting that the radio access technology determines the required  
140 received power [4].

We assume that the transmission powers and biases of the BSs in each tier are the same. Users are mobile and are subject to the inter- and intra- handovers between the cells. When a user enters a cell in tier- $j$  from tier- $k$ , we say a type  $kj$  handover occurs. Note that the number of type  $kj$  handovers is not  
145 necessarily equal to those of type  $jk$ . We assume that the total number of type  $kj$  handovers is equal to the number of times the users' trajectories cross the boundary of cells between  $k$  to  $j$ . For example, in Fig. 1.c, a 3-tier network with a hypothetical user trajectory is shown, and the numbers of handovers of type 12, 13, 21, 23, 31, 32, and 33 are equal to 1, 2, 1, 3, 2, 2, and 1.

To consider the user's mobility, we suggest a data-driven modified random  
150 waypoint model in which the distributions of the velocity, move length, and pause time are computed according to real data sets of mobile equipment, as discussed in Section 3. The objective is to estimate the handover rate of each user and for the network. Specifically, we are interested in finding how a more  
155 realistic data-driven mobility model affects the handover rate.

### 3. Mobility model

Many studies use RWP mobility to model the movement of users in the network [20, 21, 22, 23]. In the general form of the RWP mobility model, each user moves between the waypoints generated randomly in the specified  
160 region. At each waypoint, each user selects a uniform distributed angle in the interval  $[0, 2\pi]$  and moves along the path determined by that angle at a random length, denoted by  $L$ . The distributions of movement length and pause times between consecutive waypoints, in general, could have any random distribution. However, for simplicity, it is often assumed that users move at a constant velocity  
165 without pause time between waypoints [4]. The authors of [5] assume that

the user’s velocity could be constant or uniformly distributed in a range, and  $L$  follows Rayleigh distribution. That is the consecutive movement lengths  $L_1, L_2, \dots$  are independent and identically distributed (iid) random variables with the cumulative distribution function (CDF)

$$P(L \leq \ell) = 1 - e^{-\mu\pi\ell^2} \quad \ell \geq 0, \quad (2)$$

170 where  $\mu$  determines the movement length at each step. The larger the value of the  $\mu$ , the shorter is the movement length at each step where  $E[L] = \frac{1}{2\sqrt{\mu}}$ .

In this work, we focus on the importance of the mobility model on the performance analysis of handover. In this regard, we analyze the handover for the case in which the distribution of movement length in each waypoint is general  
175 with an average  $E[L]$ . We consider drivers and pedestrians as two significant groups of mobile users in the network and derive their mobility model using real traces of data.

For pedestrian users, we use real data from [24] in which the human mobility traces are collected from five different sites, including two university campuses  
180 (NCSU and KAIST), New York City, Disney World (Orlando), and North Carolina state fair. Each record of data shows the location of a pedestrian user in thirty seconds intervals, and we assume that the user has not changed her or his direction or stopped in this short intervals. For drivers, we use data of [25] in which the GPS coordinates of approximately 320 taxis collected in every seven  
185 seconds for over 30 days.

We remove outliers by considering the maximum possible speed of the pedestrians or drivers in the urban areas. We also assume that the direction of movement does not change in two consecutive intervals if the direction change is less than five degrees. Collecting the samples of the movement lengths, pause  
190 times, and speeds for each group of users, we use three goodness of fit for statistical models, including Kolmogorov-Smirnov, Anderson-Darling, and Chi-squared using to identify the best-fitted probability density function (pdf) among sixty continuous pdfs [26].

Finally, we select the pdfs with the best scores for each group of users in all  
195 three methods. We find that for pedestrians, the velocity, movement length, and  
pause time are, respectively, well modeled by Gamma, exponential, and Weibull  
distribution. For drivers, we find that the velocity, movement length, and pause  
time are best characterized by, respectively, Weibull, Gamma, and log-normal  
distributions. Fig. (2) shows the real data histogram and the selected pdfs and  
200 Table 1 shows the parameters of the considered pdfs for each group of users.  
This data analysis suggests that users' mobility profiles could not be modeled  
by simple pdfs, as assumed in many studies for simple analysis. Therefore, we  
need new tools to analyze the handover rate in more realistic scenarios.

Table 1: The mobility model parameters for pedestrians and drivers

factor	pedestrians	drivers
velocity	Gamma, $f_V(v) = \frac{v^{\alpha-1}}{\beta^\alpha \Gamma(\alpha)} e^{-\frac{v}{\beta}}$ , $\alpha = 2.51, \beta = 0.91$	Weibull, $f_V(v) = \frac{\alpha}{\beta} \left(\frac{v}{\beta}\right)^{\alpha-1} e^{-\left(\frac{v}{\beta}\right)^\alpha}$ , $\alpha = 0.83, \beta = 18.13$
move length	Exp., $f_L(l) = \alpha e^{-\alpha l}$ , $\alpha = 0.07$	Gamma, $f_L(l) = \frac{l^{\alpha-1}}{\beta^\alpha \Gamma(\alpha)} e^{-\frac{l}{\beta}}$ , , $\alpha = 169.11, \beta = 0.45$
pause time	Weibull, $f_S(s) = \frac{\alpha}{\beta} \left(\frac{s}{\beta}\right)^{\alpha-1} e^{-\left(\frac{s}{\beta}\right)^\alpha}$ , $\alpha = 0.66, \beta = 199.4$	log-normal, $f_S(s) = \frac{1}{s\sigma\sqrt{2\pi}} e^{-\frac{1}{2}\left(\frac{\ln s - \mu}{\sigma}\right)^2}$ , $\mu = 3.04, \sigma = 0.78$

#### 4. Handover analysis with modified mobility models

205 We aim to figure out the effect of the mobility model on the handover rates  
in the HWNs. Recall that the locations of BSs and hence the cells' shapes  
in a HetNet are random. We start by restating the results of [4] and [5] in  
which the users' velocities are constant, and users have nonstop moving in the  
network. Using stochastic geometry to obtain the density of cell boundaries and  
210 the intersection with user trajectory the total handover rate  $H$  and the rate of  
type- $kj$  handovers  $H_{kj}$  are derived as

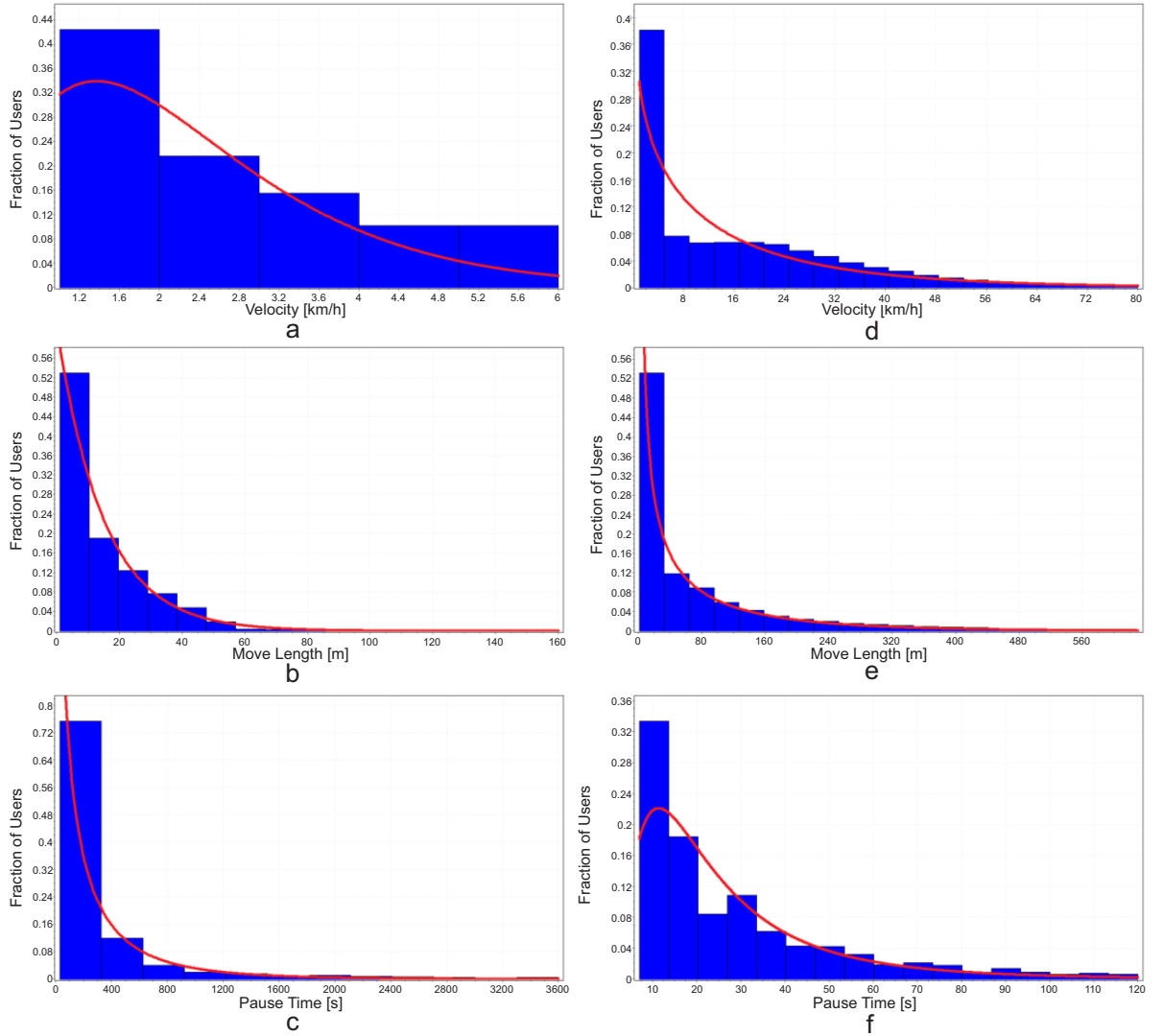


Figure 2: The best-fitted models on real data sets for the velocity, movement length, and pause time of drivers and pedestrians show different behaviors. The best fitted pdfs for velocity, move length, and pause time for pedestrians are shown in (a) to (c) and for drivers in (d) to (f). See Table 1 for parameters of each model.

$$H(v) = \frac{2E[\ell]}{\pi E[T_p]} \sum_{k=1}^K \frac{\lambda_k \left( \sum_{i=1}^K \lambda_i F(\Psi_{ki}) \right)}{2 \left( \sum_{i=1}^K \lambda_i \Psi_{ik}^2 \right)^{3/2}}, \quad (3)$$

$$H(v)_{kj} = \begin{cases} \frac{E[\ell]}{\pi E[T_p]} \left( \frac{\lambda_k (\lambda_j F(\Psi_{kj}))}{2 \left( \sum_{i=1}^K \lambda_i \Psi_{ik}^2 \right)^{3/2}} + \frac{\lambda_j (\lambda_k F(\Psi_{jk}))}{2 \left( \sum_{i=1}^K \lambda_i \Psi_{ij}^2 \right)^{3/2}} \right) & \text{if } k \neq j \\ \frac{2E[\ell] \lambda_k^2 F(1)}{\pi E[T_p] \left( \sum_{i=1}^K \lambda_i \Psi_{ik}^2 \right)^{3/2}} & \text{if } k = j \end{cases} \quad (4)$$

$$\Psi_{kj} = \left( \frac{P_k B_k}{P_j B_j} \right)^{\frac{1}{\gamma}}, \quad (5)$$

$$F(\Psi) \triangleq \frac{1}{\Psi^2} \int_0^\pi d\theta \sqrt{(\Psi^2 + 1) - 2\Psi \cos \theta}, \quad (6)$$

The network parameters in these equations include the density of BSs per tier,  $\lambda$ , the transmission power per tier,  $P$ , and the bias coefficient per tier,  $B$ . In the next section, we examine the effect of some of these parameters on the handover rate. Note that in (3) and (4), the only user related parameter is velocity  $v$ , which is directly proportional to the rate of handover. We expect to have more user-specific parameters in the estimated handover rates by more exact modeling of users' mobility. In the following, we provide the analysis which extends the analysis behind (3) and (4) and takes into account the movement length and pause time as well.

Assume that a user selects a waypoint and moves along that waypoint for  $T$  seconds and then pauses for  $S$  seconds. Let  $T_p = T + S$  denote the total time of this pass. Note that  $T$  and  $S$  are random variables. We have:

$$E[T_p] = E[T] + E[S] = E\left[\frac{L}{V}\right] + E[S] = E[L] E\left[\frac{1}{V}\right] + E[S], \quad (7)$$

where  $V$  is the random variable denoting the speed of movement and is considered independent of the movement length. We can not calculate the exact value of  $E\left[\frac{1}{V}\right]$ , analytically for the general distribution of  $V$  except for simple pdfs like uniform distribution. Instead, we use the Taylor approximation if the pdf of velocity has finite mean  $\mu$  and variance  $\sigma^2$ . We have:

$$E \left[ \frac{1}{V} \right] \approx \frac{1}{\mu} + \frac{\sigma^2}{\mu^3} \quad (8)$$

$$E [T_p] \approx E[L] \left( \frac{1}{\mu} + \frac{\sigma^2}{\mu^3} \right) + E[S] \quad (9)$$

Using (9) in (4), the handover rate of type  $kj$  is given by:

$$H_{kj} = \begin{cases} \frac{\frac{E[\ell]}{\pi} \left( \frac{\lambda_k (\lambda_j F(\Psi_{kj}))}{2(\sum_{i=1}^K \lambda_i \Psi_{ik}^2)^{3/2}} + \frac{\lambda_j (\lambda_k F(\Psi_{jk}))}{2(\sum_{i=1}^K \lambda_i \Psi_{ij}^2)^{3/2}} \right)}{E[\ell] \left( \frac{1}{\mu} + \frac{\sigma^2}{\mu^3} \right) + E[S]} & \text{if } k \neq j \\ \frac{\frac{2E[\ell] \lambda_k^2 F(1)}{2\pi (\sum_{i=1}^K \lambda_i \Psi_{ik}^2)^{3/2}}}{E[\ell] \left( \frac{1}{\mu} + \frac{\sigma^2}{\mu^3} \right) + E[S]} & \text{if } k = j \end{cases} \quad (10)$$

Next, we find the cumulative distribution function (CDF) of the handover rate using the estimated CDFs for the users' velocities. Using (3), we have:

$$H(v) = \frac{\frac{2E[\ell]}{\pi} \sum_{k=1}^K \frac{\lambda_k (\sum_{i=1}^K \lambda_i F(\Psi_{ki}))}{2(\sum_{i=1}^K \lambda_i \Psi_{ik}^2)^{3/2}}}{\frac{E[\ell]}{v} + E[S]} = \frac{\ell m v}{\ell + s v}, \quad (11)$$

where  $\ell = E[L]$ ,  $s = E[S]$ ,  $m = \frac{1}{\pi} \sum_{k=1}^K \frac{\lambda_k (\sum_{i=1}^K \lambda_i F(\Psi_{ki}))}{(\sum_{i=1}^K \lambda_i \Psi_{ik}^2)^{3/2}}$ .

To calculate the cumulative distribution function (CDF) of total handover rate, we have

$$F_H(h) = P(H < h) = P \left( \frac{\ell m v}{\ell + s v} < h \right) = P \left( v < \frac{lh}{ml - sh} \right) = F_V \left( \frac{lh}{ml - sh} \right). \quad (12)$$

Therefore, for drivers with Weibull distributed velocity model,  $F_H(h)$  is given by

$$F_H(h) = 1 - e^{-\left(\frac{1}{\beta} \left(\frac{\ell h}{ml - sh}\right)\right)^\alpha}, \alpha = 3.83, \beta = 18.13, \quad (13)$$

and for pedestrians with Gamma distributed velocity, we have

$$F_H(h) = \frac{\Gamma_{\frac{lh}{(ml - sh)\beta}}(\alpha)}{\Gamma(\alpha)}, \alpha = 2.51, \beta = 0.90 \quad (14)$$

$$\Gamma_x(\alpha) = \int_0^x t^{\alpha-1} e^{-t} dt \quad (\alpha > 0)$$

In the special case that the users' pause times are zero, the handover rate for drivers and pedestrians are, respectively, given by  $F_H(h) = 1 - e^{-\left(\frac{h}{m\beta}\right)^\alpha}$  and

$$F_H(h) = \frac{\Gamma_{\frac{h}{m\beta}}(\alpha)}{\Gamma(\alpha)}.$$

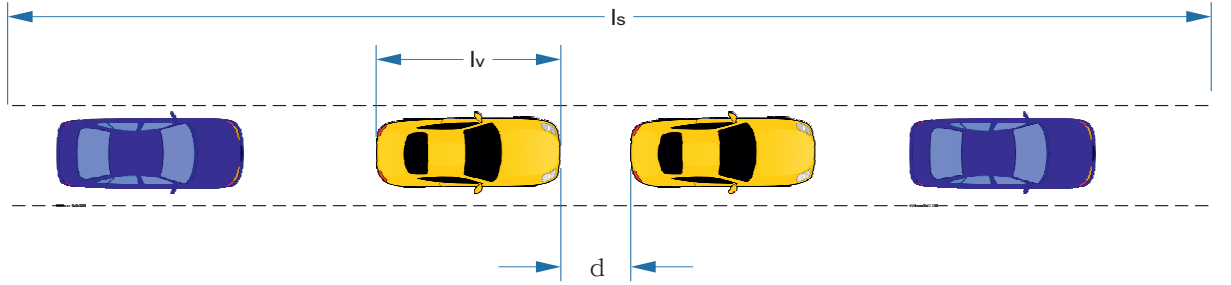


Figure 3: The number of vehicles in a lane and their velocities are dependent. The length of the lane is  $l_s$ , and the safety distance is  $d$ .

We are also interested in finding the relationship between the number of users and the handover rate, especially for a large number of users. A commonly adopted method is to compute the number of handovers for a single user and multiply that by the number of users. However, for the case of drivers, the speed  
 235 of driving and the number of drivers are not independent as each driver should maintain a safe trailing distance at any speed. For example, the well known two-second rule indicates that a driver should ideally stay at least two seconds behind any vehicle that is directly in front of his or her vehicle. Therefore, there is a nonlinear relationship between the number of drivers  $n$  and their speed  $v$   
 240 in urban areas. More specifically, assume that the average length of a vehicle is  $l_v$  meter, every vehicle has  $N_p$  passenger, and any side of the two-way highway has  $N_s$  lanes. Also, in a  $l_s$  meters long route, assume that  $N_v$  represents the number of cars and  $d$  is the distance between two cars in each lane. See figure (3). We have  $d = 2 * v$ , and therefore we can obtain a rule of thumb for the  
 245 speed and number of users as

$$N_v = \frac{2l_s N_s}{2v + l_v}, \quad n = N_p N_v = \frac{2l_s N_s N_p}{2v + l_v}. \quad (15)$$

Using (11) and (15) and assuming that users are moving at the maximum allowed speed, we can calculate the handover rate for a different number of users.

## 5. Simulations and results

250 We first consider 2- and 3-tier networks with the same bias values  $B_1 = B_2 = B_3 = 1$ , and different power levels  $P_1 = 30$  dBm,  $P_2 = 20$  dBm and  $P_3 = 10$  dBm and investigate the handover rate separately for pedestrians and drivers. The intensity of BSs in the areas that pedestrians get services are considered as  $\lambda_1 = \lambda_2 = \lambda_3 = 1$  BS/1000m<sup>2</sup> and the density of BSs in the drivers areas  
255 are considered sparser as  $\lambda_1 = \lambda_2 = \lambda_3 = 1$  BS/km<sup>2</sup>. Then, according to the defined scenarios, we change the network parameters and investigate the handover rate changes. We use the models of Table 1 to find the trajectory of each user in the network. For a fair comparison study, we also consider a scenario with driver users who follow an RWP mobility model in which the  
260 velocity of users is equal to the average velocity of our scenario.

Each user associates to the BS with the greatest biased received power according to (1). We check the users' positions in small enough time intervals to ensure capturing all possible handovers. We find out that if we reduce the time interval to less than 0.1 seconds, the handover rate obtained does not change  
265 much. Therefore, we reconsider each user's position every 0.1 seconds and update the number of handovers if the assigned BS is changed. The results are the average of the number of handovers for each user in 60 minutes. This process is repeated 300 times for each point, and we average the obtained data. The numerical results are compared against the analysis in (10) and (11).

270 In the first scenario, we investigate how the number of handovers changes as the intensity of BSs of tier-2,  $\lambda_2$ , in a 2- or 3-tier network increases. See figures (4) and (5). We have calculated the rate of handover for driver and pedestrian users, and also standard RWP. Because in all three models of user movement, a similar network model is used, the trend of change in the rate of handover  
275 is the same. However, while the density of BSs for the driver scenarios, i.e., using our mobility model and standard RWP model, is the same, the number of handovers is overestimated using the RWP model. The reason is that the RWP model calculates the time of passage much less than the actual value. In

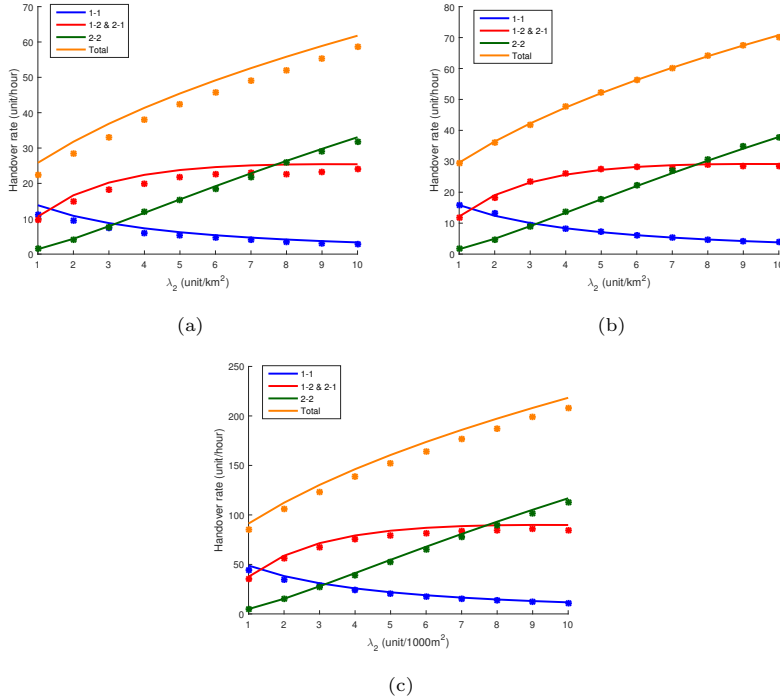


Figure 4: Variations in the handover rate against the intensity of BSs in tier-2 in a 2-tier HWN are depicted. Solid lines are the analytical results, and symbols show the numerical simulation for a specific type of a handover. (a) for drivers with the suggested mobility model, (b) for drivers with standard RWP model, and (c) for pedestrians with the suggested mobility model.

another conclusion, we found that generally, with increasing the number of BSs  
of tier- $i$ , the number of type- $ii$  handover increases linearly, and the number of  
280 type- $ij$ ,  $\{j \neq i\}$  handovers increases logarithmically and asymptotically become  
a constant value. Also, the number of handovers of type- $jk$ ,  $\{j, k \neq i\}$  decreases,  
and asymptotically become zero. The reason is that as the number of BSs at  
a given tier increases, more of the network requests are responded by BSs at  
285 that tier. That is, users either move between cells at that tier or rarely between  
cells at that tier and other tiers. Therefore, if the policy of a wireless network  
operator is to reduce the rate of inter handover at the cost of increasing the intra  
handover in a specific tier and total handover, it can increase the BS intensity

in that tier. However, if it wants to set a certain threshold for the number of  
 290 handovers in the network, it needs to have a detailed analysis of how users of  
 that network move.

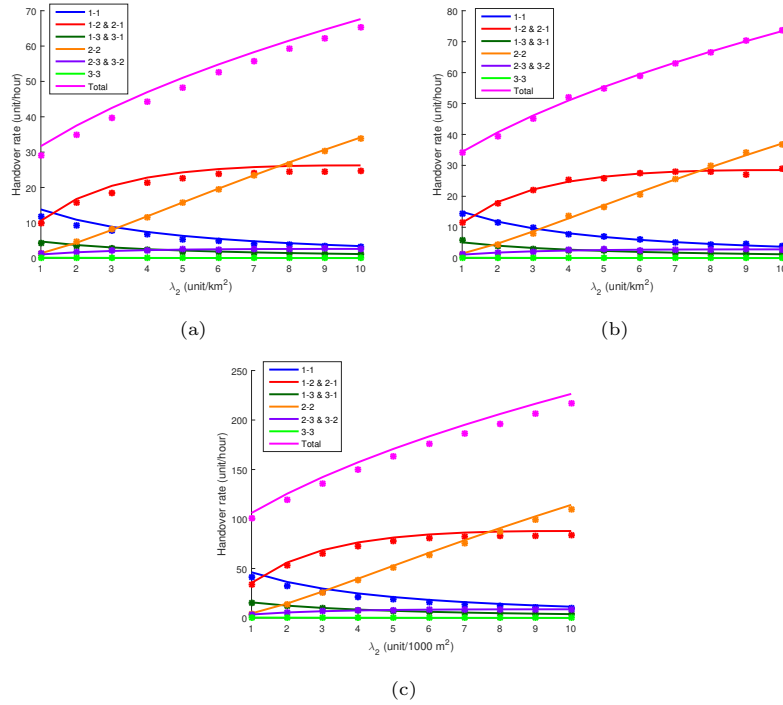


Figure 5: Variations in the handover rate against the intensity of BSs in tier-2 in a 3-tier HWN are depicted. Solid lines are the analytical results, and symbols show the numerical simulation for a specific type of a handover with the same color. (a) For drivers with the suggested mobility model, (b) for drivers with standard RWP mobility model, and (c) for pedestrians with the suggested mobility model.

In the next experiment, we investigate the effect of changing the bias value on the number of handovers with different mobility models. To do this, we modified the bias value of the BSs of tier-2 in the 2-tier and 3-tier networks and  
 295 investigated the handover rate changes. See figures (6) and (7).

As figures (6) and (7) show, the standard RWP model overestimates the handover rate. In standard RWP model, user speed is assumed to be constant and hence  $E[\frac{1}{v}] = \frac{1}{E[v]}$ . However, when the user's velocity is stochastic with

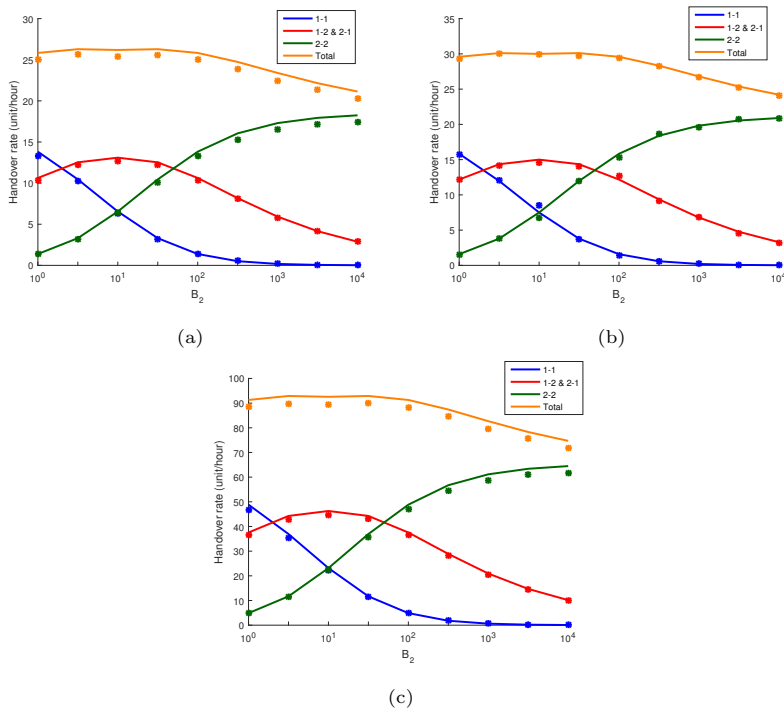


Figure 6: Variations in the handover rate against the bias value of BSs in tier-2 in a 2-tier HWN are depicted. Solid lines are the analytical results, and symbols show the numerical simulation for a specific type of a handover with the same color. (a) For drivers with the suggested mobility model, (b) for drivers with standard RWP mobility model, and (c) for pedestrians with the suggested mobility model.

a certain variance  $E[\frac{1}{v}]$  is greater than  $\frac{1}{E[v]}$  according to (8). Therefore, using  
 300 (10), the calculated value for handover decreases compared with the constant  
 velocity scenario.

Also, as the bias value of the tier-2 increases, the intra handover rate in  
 tier-2 increases. The reason is that the BSs at this tier now covers a larger area  
 of the network. However, the total number of handover decreases, because the  
 305 cells' diameters increase as well. Note that we could make the network load  
 more balanced by proper adjusting of bias values. That is, we can logically  
 move users from a crowded tier to a less crowded one. Therefore, one should  
 tradeoff between the handover rate and load balancing in different tiers of the

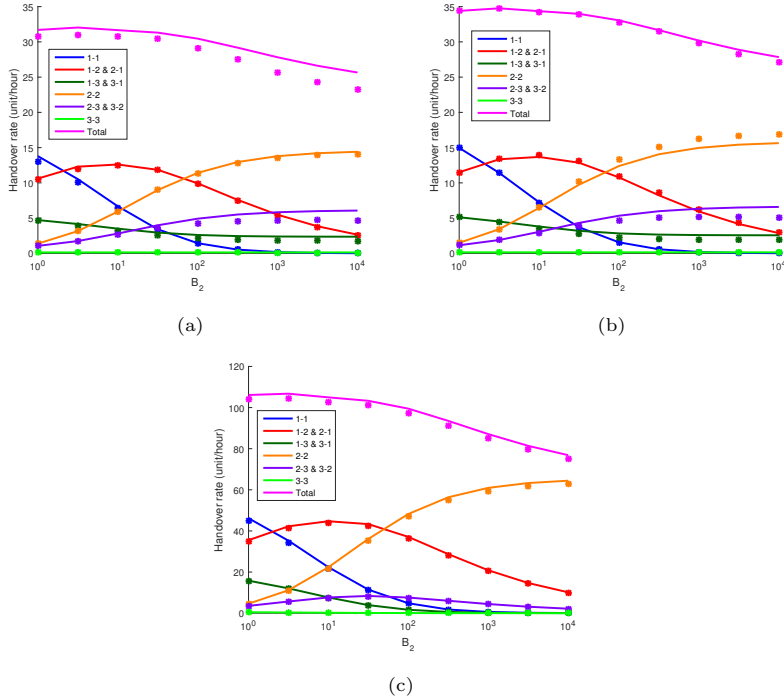


Figure 7: Variations in the handover rate against the bias value of BSs in tier-2 in a 3-tier HWN are depicted. Solid lines are the analytical results, and symbols show the numerical simulation for a specific type of a handover with the same color. (a) For drivers with the suggested mobility model, (b) for drivers with standard RWP mobility model, and (c) for pedestrians with the suggested mobility model.

network.

310 Next, we are interested in comparing how the number of tiers affects the handover rate. In Fig.8, we provide the handover rates for a 2-tier and a 3-tier HWNs where the density of BSs in the tier-2 increases. This result shows that there is a slight difference between these two scenarios. The reason is that the total number of BSs in both networks is the same, and the number of times that  
 315 a user crosses the cells' boundaries are equal in a specific route.

Finally, we investigate how the total number of handovers is changing against the number of drivers on a highway, as in Fig. (3). By assuming that the length of a vehicle is 4.5-meter, every vehicle has two passengers, and any side of a

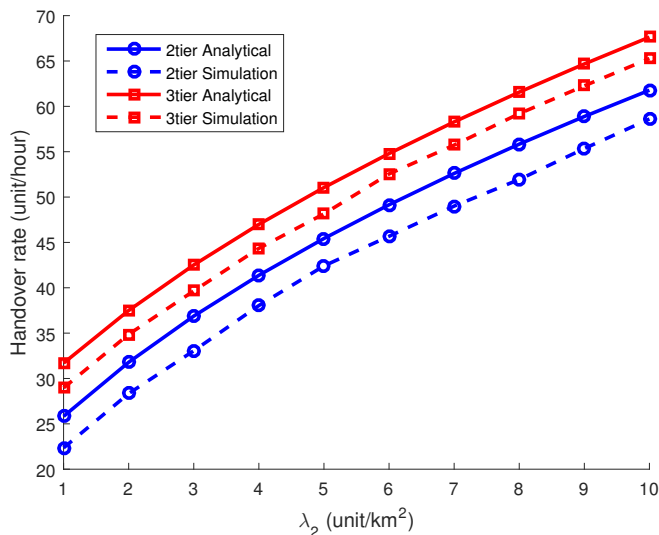


Figure 8: Comparing the handover rate of drivers in a 2-tier and 3-tier HNW against the intensity of BSs in tier-2

two-way highway has three lanes, in a 1000 meter long route, we show the  
 320 relationship between number of users and handover rate in Fig.9.

We find that in this scenario, the number of handover increases linearly as  
 the number of users increases up to a threshold corresponds to the maximum  
 allowable speed,  $80\text{ km/h}$ , as expected by (15). However, beyond that threshold,  
 the speed of users is limited, which leads to a decrease in the handover rate.

## 325 6. Conclusion

We present equations for estimating the rate of handovers in heterogeneous  
 networks. We use real data analysis to more accurately model the movements  
 of drivers and pedestrians and use these models to estimate the handover rate  
 in real scenarios better. We show that the standard RWP model overestimates  
 330 the rate of handover. Also, we show that the handover rate does not increase  
 linearly as the number of users increases. In future work, we consider a more  
 detailed analysis of the users' movements to better estimate the handover rate.

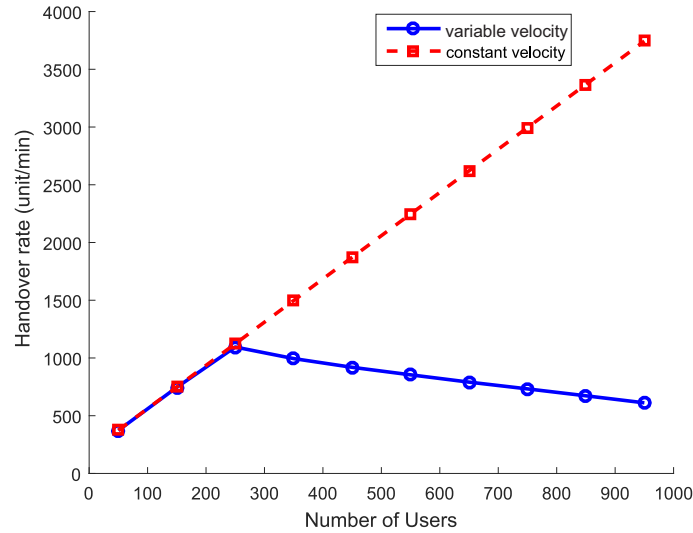


Figure 9: The relationship between the number of users and the handover rate

## References

- [1] J. G. Andrews, H. Claussen, M. Dohler, S. Rangan, M. C. Reed, Femtocells:  
 335 Past, present, and future, *IEEE Journal on Selected Areas in communications* 30 (3) (2012) 497–508.
- [2] J. G. Andrews, S. Singh, Q. Ye, X. Lin, H. S. Dhillon, An overview of  
 load balancing in hetnets: Old myths and open problems, *IEEE Wireless  
 Communications* 21 (2) (2014) 18–25.
- 340 [3] M. Stemm, R. H. Katz, Vertical handoffs in wireless overlay networks,  
*Mobile Networks and applications* 3 (4) (1998) 335–350.
- [4] W. Bao, B. Liang, Handoff rate analysis in heterogeneous cellular networks:  
 A stochastic geometric approach, in: *Proceedings of the 17th ACM inter-  
 national conference on Modeling, analysis and simulation of wireless and  
 345 mobile systems*, 2014, pp. 95–102.
- [5] X. Lin, R. K. Ganti, P. J. Fleming, J. G. Andrews, Towards understanding

the fundamentals of mobility in cellular networks, *IEEE Transactions on Wireless Communications* 12 (4) (2013) 1686–1698.

- [6] W. Bao, B. Liang, Handoff rate analysis in heterogeneous wireless networks with poisson and poisson cluster patterns, in: *Proceedings of the 16th ACM International Symposium on Mobile Ad Hoc Networking and Computing*, 2015, pp. 77–86.
- [7] S. Sadr, R. S. Adve, Handoff rate and coverage analysis in multi-tier heterogeneous networks, *IEEE Transactions on Wireless Communications* 14 (5) (2015) 2626–2638.
- [8] K. Tokuyama, N. Miyoshi, Data rate and handoff rate analysis for user mobility in cellular networks, in: *2018 IEEE Wireless Communications and Networking Conference (WCNC)*, IEEE, 2018, pp. 1–6.
- [9] R. Arshad, H. ElSawy, L. Lampe, M. J. Hossain, Handover rate characterization in 3d ultra-dense heterogeneous networks, *IEEE Transactions on Vehicular Technology* 68 (10) (2019) 10340–10345.
- [10] T. M. Duong, S. Kwon, Vertical handover analysis for randomly deployed small cells in heterogeneous networks, *IEEE Transactions on Wireless Communications* 19 (4) (2020) 2282–2292.
- [11] M. M. U. Chowdhury, P. Sinha, I. Guvenc, Handover-count based velocity estimation of cellular-connected uavs, *arXiv preprint arXiv:2002.06657*.
- [12] W. Bao, B. Liang, Stochastic geometric analysis of user mobility in heterogeneous wireless networks, *IEEE Journal on Selected Areas in Communications* 33 (10) (2015) 2212–2225.
- [13] F. Baccelli, M. Klein, M. Lebourges, S. Zuyev, Stochastic geometry and architecture of communication networks, *Telecommunication Systems* 7 (1-3) (1997) 209–227.

- [14] M. Haenggi, J. G. Andrews, F. Baccelli, O. Dousse, M. Franceschetti, Stochastic geometry and random graphs for the analysis and design of wireless networks, *IEEE journal on selected areas in communications* 27 (7) (2009) 1029–1046.
- [15] D. Moltchanov, Distance distributions in random networks, *Ad Hoc Networks* 10 (6) (2012) 1146–1166.
- [16] J. G. Andrews, F. Baccelli, R. K. Ganti, A tractable approach to coverage and rate in cellular networks, *IEEE Transactions on communications* 59 (11) (2011) 3122–3134.
- [17] H.-S. Jo, Y. J. Sang, P. Xia, J. G. Andrews, Heterogeneous cellular networks with flexible cell association: A comprehensive downlink sinr analysis, *IEEE Transactions on Wireless Communications* 11 (10) (2012) 3484–3495.
- [18] Y. Lin, W. Yu, Optimizing user association and frequency reuse for heterogeneous network under stochastic model, in: 2013 IEEE global communications conference (GLOBECOM), IEEE, 2013, pp. 2045–2050.
- [19] S. Singh, H. S. Dhillon, J. G. Andrews, Offloading in heterogeneous networks: Modeling, analysis, and design insights, *IEEE Transactions on Wireless Communications* 12 (5) (2013) 2484–2497.
- [20] C. Bettstetter, H. Hartenstein, X. Pérez-Costa, Stochastic properties of the random waypoint mobility model, *Wireless Networks* 10 (5) (2004) 555–567.
- [21] G. Resta, P. Santi, An analysis of the node spatial distribution of the random waypoint mobility model for ad hoc networks, in: Proceedings of the second ACM international workshop on Principles of mobile computing, 2002, pp. 44–50.
- [22] C. Bettstetter, G. Resta, P. Santi, The node distribution of the random waypoint mobility model for wireless ad hoc networks, *IEEE Transactions on mobile computing* 2 (3) (2003) 257–269.

- [23] E. Hyytia, P. Lassila, J. Virtamo, Spatial node distribution of the random waypoint mobility model with applications, *IEEE Transactions on mobile computing* 5 (6) (2006) 680–694.
- [24] I. Rhee, M. Shin, S. Hong, K. Lee, S. Kim, S. Chong, Crawdad data set  
405 ncsu/mobilitymodels (v. 2009-07-23) (2009).
- [25] L. Bracciale, M. Bonola, P. Loreti, G. Bianchi, R. Amici, A. Rabuffi, Crawdad dataset roma/taxi (v. 2014-07-17), CRAWDAD wireless network data archive.
- [26] EasyFit version 5.5, <http://www.mathwave.com/easyfit-distribution-fitting.html>,  
410 accessed: 2020-03-03.